Air-Sea Exchange in Hurricanes: Synthesis of Observations from the Coupled Boundary Layer Air-Sea Transfer Experiment

Peter G. Black[1*], Eric A. D'Asaro[2], William M. Drennan[3], Jeffrey R. French[4], Pearn P. Niiler[5], Thomas B. Sanford[2], Eric J. Terrill[5], Edward J. Walsh[6] and Jun Zhang[3]

[1]NOAA/AOML Hurricane Research Division, Miami, Florida

[2]University of Washington, Applied Physics Laboratory, Seattle Washington

[3]University of Miami, Rosenstiel School of Marine and Atmospheric Science, Miami, Florida

[4,]University of Wyoming, Department of Atmospheric Science, Laramie, Wyoming

[5]University of California, Scripps Institution for Oceanography, La Jolla, California

[6]NASA, Goddard Space Flight Center, Wallops Island, Virginia

Submitted to BAMS

March 2006

* *Corresponding author address:* Peter G. Black, NOAA/AOML Hurricane Research Division, Miami, FL 33149
E-mail peter.black@noaa.gov

Combining airborne remote, in-situ and expendable probe sensors with air-deployed ocean surface platforms provides an observational strategy for expanded knowledge of illusive high wind air-sea flux observations from hurricanes imbedded in difficult-to-predict, large-scale atmospheric weather patterns.

1. Introduction

The Coupled Boundary Layer Air-Sea Transfer (CBLAST) experiment was conducted during 2000-2005 to improve our fundamental understanding of physical processes at the air-sea interface. We focus here on the CBLAST-Hurricane component which included experimental observations of the air-sea exchange process in high winds suitable for improving hurricane track and intensity model physics. Other CBLAST activities focused on low wind dynamics (Edson et al 2006) and modeling (Chen et al 2006).

Energy exchange at the air-sea interface is one of three major physical processes governing hurricane intensity change. The others are environmental interactions with surrounding large scale features in the atmosphere and internal dynamics such as eyewall replacement cycles and cloud microphysics. The air-sea exchange of heat, moisture and momentum determines how hurricanes gain their strength and intensity from the ocean. This has become an extremely important problem over the past several years as we have entered a new era of greater numbers of hurricanes (Goldenberg, 1998), as well as an era of more intense hurricanes (Emanuel, 2005; Webster et al., 2005). The past two years have witnessed an increase in the number of major hurricane landfalls. While efforts to forecast hurricane track have improved greatly over the past 15 years, our ability to forecast hurricane intensity has shown little skill (DeMaria et al., 2005). With more hurricane threats on the U. S. and Caribbean coastlines, the effort to improve hurricane intensity forecasting has taken on greater urgency. The mitigation actions that are taken by emergency management officials, local, state and federal governments and private industry all depend on predictions of intensity thresholds at and near

landfall. In response to this need for improved hurricane intensity forecasts, the Office of Naval Research (ONR) initiated the CBLAST program.

The resulting CBLAST Hurricane experiment became a cooperative undertaking between the ONR, NOAA's Office of Oceanic and Atmospheric Research (OAR), Hurricane Research Division (HRD), Aircraft Operations Center (AOC), including it's United States Weather Research Program (USWRP) and the United States Air Force Reserve Command's 53rd Weather Reconnaissance Squadron (AFRC) . ONR provided support for 17 PI's (see Table 1) from universities and government laboratories. NOAA provided aircraft flight hour support for two WP-3D research aircraft, expendable probes and Hurricane Field Program infrastructure. AFRC, through the 53rd Weather Reconnaissance Squadron, provided infrastructure support, specialized expertise in air deployment of large platforms and WC-130J and C-130J aircraft support. The observational strategies and initial results of this effort are described in the following pages.

The overarching goal of CBLAST was to provide new physical understanding that would improve forecasting of hurricane intensity change with the new suite of operational models now undergoing testing and evaluation at the Naval Research Laboratory (NRL) and at NOAA's Environmental Modeling Center (EMC). CBLAST focused an intensive effort on observing air-sea interaction processes within hurricanes because of the recognized lack of knowledge of the physics of air-sea exchange at winds above gale force. Prior to CBLAST, no in-situ air-sea flux measurements existed at wind speed above 22 m/s. Parameterization schemes used to approximate air-sea transfer at hurricane wind speeds were simply an extrapolation of low wind measurements with the assumption that the physical processes were the same – despite clear visible evidence to the contrary! A goal of CBLAST was to extend the range of observations for

exchange coefficients of momentum, heat and moisture across the air-sea interface during hurricane force winds.

2. CBLAST Concept and Observation Plan

The CBLAST experimental design consisted of two major observational components: 1) airborne in-situ and remote sensing instrumentation flown into hurricanes by the two NOAA WP-3D aircraft and 2) air-deployed surface drifting buoys and subsurface profiling floats. This was intended to provide a mix of 'snapshots' of inner-core hurricane conditions each day over a 2-4 day period together with a continuous time series of events at particular ocean locations. A third component, available based on operational needs, consisted of the hurricane synoptic surveillance program designed for improved track forecasting. It provided, on occasion, concurrent high-level NOAA G-IV jet aircraft flights in the hurricane environment, deploying GPS dropsondes to profile the steering currents and significant synoptic features, in addition to reconnaissance flights within the hurricane's inner core from the WC-130H operated by AFRC 53rd WRS. Polar-orbiting and geostationary satellite platforms provided additional remote sensing measurements in the hurricane's inner core and environment.

The aircraft component of CBLAST had two modules: a) an aircraft stepped descent module and b) an inner-core survey module. The former was designed to focus on in-situ air-sea flux and spray measurements, while the latter was to focus on large-scale structure, eyewall flux budget measurements and documentation of internal dynamics. The centerpiece of this effort involved a multi-sonde sequence of 8-12 GPS dropsondes dropped from coordinated WP-3Ds flying in tandem at different altitudes. See Fig. 1 for a schematic of a typical flight plan. Each module consisted of several options related to precise experiment patterns dictated by prevailing

conditions and available time on station. For instance, the stepped descents (Fig. 2), down to as low as 70m above the sea, were only carried out in clear air conditions between rainbands.

Both modules were complemented with an array of airborne remote and in-situ sensors. Air-deployed drifting buoys and oceanographic floats (auto-profiling oceanographic radiosondes) were designed to further complement the airborne in-situ and remote sensing of the air-sea interface. This air-deployment module consisted of arrays of sensors measuring continuous time series of surface and upper ocean conditions before, during and after hurricane passage. Together the aircraft and buoy/float array provided a unique description of air-sea fluxes, surface wave and upper ocean conditions in hurricane conditions never before achieved. The synoptic surveillance program provided observations on cases where environmental interactions were important, allowing research efforts to distinguish between intensity changes resulting from air-sea interaction processes and those resulting from environmental interactions with significant synoptic scale features in the near-storm environment. In a similar fashion, the inner core survey module provided observations of significant changes in the inner core dynamics occurring concurrently with observed air-sea processes. In principle this was to provide an overarching data base to allow intensity changes from air-sea interaction causes to be separable from those due to environmental interactions and internal dynamics.

3. Case Studies

The CBLAST experimental effort began in 2000 with the development of six new airborne instrument systems, three new oceanographic float designs, 2 drifting buoy designs, the flight pattern strategy and the air-deployment strategy, including the WC-130J air-deployment certification and air-drop certification of 3 platform types. The new airborne instrument systems

were 1) Best Atmospheric Turbulence (BAT) probe for fast response temperature and u,v,w wind components, 2) LICOR fast response humidity system, 3) CIP particle spectrometer and 4) Particle Doppler Analyzer (PDA) for sea spray droplet observation, 5) Downward-looking MASS high-speed visible and infrared camera systems for wave breaking observations, 5) Scanning Radar Altimeter (SRA) for directional wave spectra, 6) Stepped and Simultaneous Frequency Microwave Radiometers (SFMR and USFMR) for surface wind speed and 7) the Integrated Wind and Rain Atmospheric Profiler (IWRAP) for continuous boundary layer and surface wind vector profiles.

These systems were built in 2001 and flight-tested in 2002. Two storms, Edouard and Isidore, were flown in 2002, the first to test the new stepped-descent flight pattern strategy and the second to test extended low level flight pattern for detection of secondary roll circulations. The CBLAST field program began in earnest in 2003 with the survey flight pattern flown on 6 days by the two NOAA WP-3D aircraft together (a total of 12 fights) with 15 stepped-descent patterns flown within the hurricane boundary layer in Hurricanes Fabian and Isabel from a staging base in St. Croix, U.S. Virgin Islands. An additional 10 AFRC WC-130H reconnaissance flights and 3 NOAA G-IV surveillance flights were also flown during this period. A 2 X 4 array of 16 drifting buoys and 4 floats were deployed by the 53rd WRS from a WC-130J aircraft (Fig 3) ahead of Hurricane Fabian. The aircraft fleet in St Croix is shown in Fig. 3- the NOAA WP-3D crew and scientists in fig. 4.

An engine failure due to salt build-up occurred near the end of the 6th flight resulted in new safety regulations requiring a chemical engine wash after each flight below 340 m. CBLAST flights in 2004 continued, but were restricted to flight levels above the boundary layer.

The CBLAST flights in 2004 were in Hurricanes Frances on 5 days, Ivan on 4 days and Jeanne on 3 days. The key success in 2004 was the air-deployment by the 53rd WRS of 38 drifting buoys (30 Minimet; 8 ADOS) and 16 floats (9 ARGO/SOLO; 2 gas flux; 2 Lagrangian; 3 EM/APEX) in Hurricane Frances.

4. Key results from the aircraft component

a. First turbulence measurements in tropical storm and hurricane force winds

The principal results from the aircraft component of CBLAST were the estimation of surface momentum and enthalpy flux from direct eddy correlation measurements of using two newly modified airborne instrument packages: the "Best Atmospheric Turbulence" Probe (BAT) and the LICOR fast response humidity probe, shown mounted on the WP-3D aircraft in Fig. 6. The results are based on measurements obtained during 15 stepped-descent patterns flown in Hurricanes Fabian and Isabel on 6 days in 2003 (Fig. 7). Details are presented in French et al (2006) and Drennan et al (2006). A total of 48 independent estimates of $C_{D,10N}$ and 42 estimates of $C_{E,10N}$ (hereafter referred to as C_D and C_E, respectively) were derived from measured fluxes and SFMR estimates of U_{10N}, the ten-m surface wind. Several surprising results emerged from these measurements. Our results indicate a leveling of C_D at wind speeds of approximately 22-23 m/s. This is a full 10 to 12 m/s less than suggested in earlier studies (Powell et al,,2003; Donelan et al, 2004; Fig. 8). Estimates of C_E above 20 m/s are in very good agreement with the HEXOS results (DeCosmo, et al., 1996) for wind speeds below 20 m/s suggesting that C_E is constant with wind speed to hurricane force conditions of approximately 33 m/s (Fig. 9).

When CBLAST C_D and C_E results are compared with other studies (Fig. 10), one can see that they represent a doubling of the wind speed range of observations previously available, which is a significant achievement. It is apparent that the CBLAST high-wind C_D values represent significant departure from prior estimates. It also becomes obvious that while CBLAST extended the range of prior observations, a further doubling of the wind speed range is required to estimate fluxes in hurricane conditions from CAT 1 to CAT 5. It is in this range that physical processes may depart significantly from moderate hurricane wind conditions as the importance of sea spray increases dramatically, a process that little is known about at present.

The new C_D and C_E observations as well as the somewhat tenuous extreme wind estimates is that the ratio of C_E/C_D, hypothesized by Emanuel (1995) to be an important parameter in estimating hurricane potential intensity, decrease to values on order of 0.5-0.75 for tropical storm and CAT 1-3 hurricane conditions before increasing to values close to 1.5 at CAT 5 conditions. This is equal to or below Emanuel's threshold for hurricane development (0.75) indicated by the horizontal line in Fig. 11. The implications of this new observation is being investigated further by Montgomery, et al., 2006.

b. Surface wave observations

The Scanning Radar Altimeter (SRA) on the P3 aircraft recorded huge data sets on the 2D wave spectra in all quadrants of CBLAST storms in 2004 and in Fabian in 2003. Typical of those results was the image in Fig. 12 from the front quadrant of Hurricane Fabian near 200 m altitude which shows the predominant 200 m swell propagating to the upper left of the image. Superimposed on the swell is the local sea with wavelengths of about 80-100 m crossing at a 90º angle and propagating toward the lower left. This is typical of conditions depicted in Fig. 13,

which illustrate 3 sectors of distinctly different 2D wave spectra, discussed by Wright, et al., 2001. The spectra in sector I tend to be tri-modal with 2 swell peaks plus the local sea. The spectra in sector II tend to transition from tri-modal to bi-modal with the swell following within 30 degrees of the local sea. The spectra in sector III tend to transition from bimodal to unimodal depending on whether the local seas is resolved. The swell tends to propagate at about a 90 degree angle to the local sea in this region.

A further illustration of the behavior of the swell relative to the local sea is shown in Fig 14, from SRA measurements throughout Hurricane Ivan (2004). Fig. 14 shows an HRD HWIND surface wind analysis- based primarily on SFMR surface wind data- for Hurricane Ivan on 14 September 2004 when Ivan was moving northwest. Twelve SRA spectra about 80 km from the eye are shown in Fig. 14. In the right-front quadrant (sector II/III boundary) the wave field is unimodal with 350 m wavelength and 11.4 m wave height. Directly to the right of the track the wavelength shortens to about 260 m and the spectrum broadens and becomes bimodal. In the right-rear quadrant the wave height decreases and the spectrum becomes trimodal. In the rear quadrant of Ivan, as was the case with Bonnie (Fig. 13), the wave height and length reach minimum values of 5.6 m and 190 m, about half their values in the right forward quadrant. This suggests the waves are young, steep and short in the right-rear quadrant and older, flatter and long in the right front and left front quadrants. To the left-rear and left-front of the eye, the wind and waves are about at right angles to each other.

The expectation was that the exchange coefficients would exhibit a variability that depended on the characteristics of the 2D wave spectrum. This has turned out to not be the case as one can see be reflecting on Figs. 7-9 and comparing these results with Fig. 14. What this says, and what emerges as the second major conclusion for CBLAST hurricane measurements, is

that surface fluxes and exchange coefficients derived from them (Figs. 8-9) appear not to be a function of the variation in the relationship between the long wavelength swell and the shorter wavelength local sea, at least at the hurricane force wind radii and greater, i.e for minimal hurricane conditions.

c. Evidence for secondary boundary layer circulations

Strong evidence was found for the existence of 'roll vortex' secondary boundary layer circulations in hurricanes. Complementing the CBLAST flights in 2002-2004 were a number of RADARSAT and ENVISAT Synthetic Aperture Radar (SAR) passes (see Fig. 15, top) over the storms which all showed streaks in the radar backscatter with wavelengths on the order of 800-1000 m. These were most prominent in the front semicircle of the storm. Spectral analysis of these images over 1km square pixels were able to retrieve a direction, found to be nearly equal to the wind direction (Katsaros, et al., 2002), as well as a wavelength. Fig. 15 (bottom) illustrates a spectrum averaged over six such 2D spectra (6 km square) that shows a peak in the spectrum near 900 m. This value is close to that determined recently by Morrison, et al., 2005 from ground-based WSR-88D Doppler radar observations in landfalling hurricanes. Their results are supported by more recent higher-resolution portable Doppler radar (SMART-R) observations in landfalling hurricanes (Losorlo, et al., 2006) and by Doppler on Wheels (DOW) high resolution portable Doppler radar observations in Hurricane Fran (Wurman and Winslow, 1998), and more recently in Hurricane Rita (2005). So these features are now well documented in landfalling hurricanes, and the satellite SAR observations suggest they are endemic to the hurricane wind field over the ocean. The significance of this observation is that these 'roll' features, and their possible major effects on air-sea fluxes as suggested by Morrison et al., 2005 and Foster, 2005, are not currently modeled in any major hurricane coupled modeling effort.

To further emphasize this observation, the u'w' vertical co-spectrum was computed from gust probe data in Hurricane Isidore (2002) along a 75 km leg flown at 300 m, near the middle of the hurricane planetary boundary layer with a lid at 500 m altitude. The first part of the leg was in the radial direction toward the eye and showed a very coherent peak in the spectrum near 900 m (Fig. 16), in close agreement with the scales from the SAR images (Fig. 15, bottom). This peak disappeared when the aircraft turned and flew along wind. Ongoing studies suggest these features may play an important role in boundary layer fluxes. This factor leads to the third major CBLAST finding to date, which is that secondary boundary layer circulations, while not a major thrust of the original CBLAST plan, and while not presently represented in existing coupled hurricane modeling efforts, are a major factor in the hurricane boundary layer flow field and are likely a major player in air-sea fluxes.

5. Key Results from the Air-Deployed Oceanographic Sensor Component of CBLAST Hurricane

The 54 buoys and floats deployed into Hurricane Frances in 2004 yielded a wealth of information on ocean structure and structure changes induced by the hurricane within and below the ocean mixed layer: the first ever 4D ocean structure observations beneath a hurricane. Detailed measurements of the ocean and air-sea interface beneath hurricanes were made using several varieties of autonomous floats and drifters that were air-deployed ahead of the storm. The technology for these devices has matured rapidly in recent years so that they are now deployed in large numbers as part of the developing system for observing the world ocean. For CBLAST, air-deployment systems were developed for existing platforms and they were equipped with new sensors to measure properties of the air-sea interface. Sufficient measurements were made to map the space-time evolution of the ocean beneath a hurricane. The goal of these investigations

was to understand the properties of the air-sea interface and upper ocean at wind speeds greater than 30 m/s, to determine the associated air-sea fluxes and the effect of these on hurricane intensification.

The region of high winds beneath a hurricane is quite small, a few hundred km in diameter for the largest storms, much less for a typical storm. Accordingly, the probability of measuring high winds from an array of instruments prepositioned in "hurricane alley" is small. As with meteorological studies of hurricanes, a viable sampling plan must rely on real-time measurements of storm position, reliable forecasts of future storm tracks and the ability of aircraft to deploy sensors in or near an active storm based on this information. Accordingly, close cooperation between the National Hurricane Center, which supplied the storm forecasts, the scientific team, who adapted the sampling array to these changing conditions, and the 53rd Air Force Reserve squadron, who deployed the instruments, was essential. Equally important was the use of UNOLS ships to recover the floats after the hurricane had passed.

The five varieties of oceanographic instruments used in CBLAST Hurricane can be divided into two categories: *drifters* and *floats*. Details of each instrument type are shown in Table 3. Fig. 17 shows drawings of each instrument and a schematic of their operation in Hurricane Frances (2004).

Drifters aim to follow the ocean current at 15m depth while measuring both near-surface atmospheric and upper-ocean properties. A small surface float supports a much larger drogue centered at 15m depth. The large drogue causes the drifter to nearly follow the horizontal water motion at approximately 15m. A transmitter in the surface drifter sends data to the ARGOS

satellite system. The same signals are used to track the drifter. The standard drifter measurements are position and near-surface temperature. The CBLAST drifters carried additional sensors. Minimet drifters are also designed to estimate wind speed using the sound level at 8 Khz (Nystuen and Selsor, 1997) and wind direction using a vane on the surface float. Evaluation of the accuracy of this approach at hurricane wind speeds is still under way. ADOS drifters additionally measure the temperature profile to 100m depth.

The three varieties of floats are shown in Fig. 17. All floats operate by mechanically changing their volume, and thus their density, in order to control their depth. By making themselves light, they can profile to the surface thereby extending an antenna out of the water enabling them to obtain a GPS fix and relay data to and receive instructions from their shore-based operators. The EM-APEX floats (Fig 17, green lines) operated as profilers, continuously cycling while measuring temperature, salinity and velocity. Profiles extended from the surface to 200m with profiles to 500m every half inertial period. During the storm, the top of the profiles terminated at 50m. The Lagrangian floats (D'Asaro, 2003), profiled only before and after the storm (Fig. 17 black line). During the storm, they remained neutrally buoyant, following the three-dimensional motion of water parcels in the highly turbulent upper boundary layer. They measured temperature, salinity and gas concentration. The SOLO floats combined profiling of temperature, salinity and oxygen from the surface to approximately 200m (Fig. 17, blue line) while hovering at about 40m for a period of time during each dive interval to remotely measure surface waves and the depth of the bubble layer created by surface wave breaking using a compact sonar, and 0-50KHz ambient sound with a passive hydrophone. The floats were programmed to repeat its dive interval every 4 hours.

Initial deployments were made in Hurricane Isidore in 2002 and Fabian in 2003. The

more extensive 2004 deployments ahead of Hurricane Frances will be described here. The array of floats and drifters (Fig 18) was deployed on Aug. 31, 2004 based on the Aug. 30, 11 pm EDT forecast. The storm track passed just north of the shallow banks and islands north of Hispaniola. The array was therefore placed over deep water north of the storm track. The forecast proved to be extremely accurate, so that array elements passed under both the eye and maximum winds (60 m/s) of the storm.

The Hurricane Frances deployments clearly demonstrated the success of this new approach to measurement in hurricanes. The instruments were accurately targeted into the CAT 4 hurricane. All of the varieties of drifters and floats survived and worked successfully in this environment, with only minimal losses. Data was transmitted from the high wind region of the hurricane in nearly real time.

The buoys and floats revealed a warm anticyclonic eddy directly in the path of the storm which was flanked by cooler cyclonic features. Sea surface height anomaly maps from satellite altimetry further indicates the presence of an eddy rich ocean in the vicinity of the storm track.

Parameterization of the air-sea fluxes that drive hurricanes depends on an understanding of the air-sea interface at high wind speeds. Figure 19 shows the ability of the floats to make detailed measurements of surface waves and near-surface bubble clouds across the hurricane. The time varying height of the sea surface was measured by the SOLO floats using an upward looking sonar compensated for the measured float depth. High frequency fluctuations in sea height yield measurements of the surface waves. Maximum significant wave height exceeded 10m. Intense breaking of these large waves injects bubbles into the ocean. The resulting near-surface bubble layer plays a key role in gas flux across the air-sea interface as well as having an important dynamical effect by changing the bulk density of the near-surface layer. Bubbles are

very efficient sound scatterers, so that the thickness of the near-surface bubble layer can be measured by the upward looking sonar. Its thickness increases approximately as wind speed cubed, reaching a maximum thickness of about 10m. These results are confirmed by Lagrangian float measurements of conductivity, which decreases in the upper 10m due to bubbles. The estimated air fraction reaches 10^{-3}, dynamically equivalent to a temperature change of 3˚C.

Hurricanes draw their energy from the warm ocean waters. However, ocean mixing beneath a hurricane can significantly reduce sea surface temperatures from the pre-storm values. Fig. 20 shows the evolution of upper ocean temperature under the strongest winds of Hurricane Frances. It combines the vertical temperature profiles from an EM-APEX float with the nearby temperature measurements from the two Lagrangian floats. The EM-APEX floats also showed the evolution of the currents in the upper ocean (Sanford, et al., 2005). Fig 21 shows rapid deepening of the mixed layer and associated high shear across the thermocline. The strong wind and wave forcing directly generates turbulence in the upper 20-40m of the ocean. The Lagrangian floats are advected by the large-eddy velocities of this turbulence, repeatedly cycling across the turbulent layer and thereby tracing its depth and intensity (red and blue lines). Turbulent velocities are 0.1 m/s rms at the height of the storm, with the strongest downward jets reaching 0.3 m/s. The turbulent layer extends to 50m at the height of the storm. However, the changes in temperature, indicate that mixing extends to 120 m (magenta line). Measurements of shear by the EM-APEX floats show (Fig. 21) a nearly critical Richardson number down to 120m, indicating a key role for shear instability in this deeper mixing. The one dimensional heat budget requires even deeper mixing as shown by the yellow dashed line. A more detailed analysis indicates that horizontal heat fluxes become important as the magenta and yellow-dashed lines diverge, indicating a transition of the boundary layer heat budget from vertical to three-

dimensional.

The net effect of this strong ocean mixing is to cool the ocean surface, potentially reducing the enthalpy flux to the hurricane. The combined data from the floats and drifters is used to map the amount of cooling in Fig. 22. Cooling is most intense to the right of the storm center, with a cold wake spreading outward behind this region. The leading edge of this wake forms an SST front approximately 50 km wide which moves with the storm. The eye of storm is at the edge of this front, so that cooling at the eye is only about 0.5˚C compared to the maximum of 2.5˚C in a crescent-shaped pattern in the storm's right-rear quadrant, similar to that proposed by Black, et al.,1988. SST gradients of up 2˚C exist across the inner 50 km of the storm, with a temperature range of about 27.5-30˚C. These data suggest that rather than specifying the SST at the hurricane inner core, it may be more useful to think in terms of the location of the SST front that exists beneath the core. Small changes in the location of this front relative to the core may have large effects on the enthalpy flux driving the storm.

6. SUMMARY AND CONCLUSIONS

CBLAST hurricane program has yielded an unprecedented data set for exploring the coupled atmosphere and ocean boundary layers during an active hurricane. Key results from the analysis effort to date have doubled the range of air-sea flux measurements, which have allowed drag and enthalpy exchange coefficients to be estimated in wind speeds up to hurricane force. The drag coefficients estimated from this work suggest a leveling off with wind speed near 22-23 m/s, a considerably lower threshold than previous studies. This results in a drag coefficient of

0.0015 for hurricane conditions in contrast with the earlier estimates of 0.0022. The Dalton number is constant with wind speed up to hurricane force with a value of 0.0011, in close agreement with lower wind HEXOS and TOGA/COARE estimates. This results in a C_E/C_D ratio of 0.7, close the Emanuel threshold for hurricane development. Directional wave measurements made from the aircraft show distinctive characteristic as a function of storm-relative quadrant. Spectra range from tri-modal in the right-rear quadrant to bi-modal in the right front to uni-modal in the left-front. The exchange coefficients appear independent of this wave spectral characteristics to within observational uncertainty. Secondary boundary layer circulations appear to characterize the boundary layer throughout the hurricane with their role in flux estimation yet to be determined.

The drifter and buoy deployments in Hurricanes Fabian (2003) and Frances (2004) were unqualified successes yielding first time ever observations of the 4-dimensional evolution of the subsurface ocean structure concurrent with airborne atmospheric boundary layer observations. The development of the cold wake behind Frances, showing a crescent-shaped pattern of cooling in the near-storm environment, was well observed with maximum cooling of 2.5 C. Shear at the base of the ocean mixed layer was found to develop quickly beneath the hurricane and exceed the Richardson Number criteria of 1/4 for onset of turbulent mixing.

The analyses of this immense data set is ongoing. Incorporation into research and operational coupled models is just beginning. The outlook for major impacts on these modeling efforts is optimistic.

7. FUTURE PLANS FOR CBLAST HURRICANE

The analysis of CBLAST hurricane data sets has just begun. Continued support for analysis efforts is being provided by ONR and NOAA through the U.S. Weather Research Program (USWRP). Additional fundamental research will be ongoing in the years ahead for efforts such as merging 2D wave spectra from the SRA and the 1D wave spectra from the ARGO/SOLO floats to estimate the high frequency portion of the wave spectrum and its impact on air-sea fluxes in hurricanes. Follow-on work will continue to better define the structure of roll vortex circulations and their role in air-sea fluxes. The impact of sea spray on air-sea enthalpy and momentum fluxes is yet to be demonstrated in hurricane extreme winds, especially for major hurricanes of CAT 3 and above. Additional analysis of the GPS sondes from the multi-sonde deployments in the hurricane eyewall for the purpose of estimating eyewall air-sea flux via budget calculations and form that and SFMR surface wind, SST and specific humidity estimates to arrive at additional C_D and C_E estimates for extreme winds in excess of 50 m/s. Work will continue on the diagnoses of boundary layer secondary circulations, i.e. 'roll vortices' and the variability by storm quadrant from additional spectral analysis of BAT and LICOR data from along and cross wind flight legs as well analysis of IWRAP boundary layer wind profiles to address vertical structure issues of this phenomenon. Continued synthesis of drift buoy, float and satellite observations of ocean features in the path of Fabian and Frances will continue, including efforts to improve ocean mixing parameterizations in hurricane conditions.

Efforts to estimate fluxes at the top of the hurricane boundary layer will begin. Using the suite of BAT and LICOR turbulence instrumentation now available for both NOAA WP-3D aircraft, additional measurements will be sought over the coming years to fill the many gaps in the CBLAST data and to continue to focus on the parameterization with wind speed, wave

conditions and roll vortex effects. These observations will accompany new observations of sea spray droplets from any possible low level flights using the new suite of cloud microphysical spectrometer probes presently being improved on the P3 aircraft- opening the possibility of extending sea spray studies.

The focus will also shift toward integrating existing and anticipated results on air-sea flux parameterization into the evolving HWRF operational model at the NOAA Environmental Prediction Center (EMC) as that model comes on line operationally and begins to build a data base with existing parameterization schemes. EMC will also be examining the benefits of assimilating the profiling float data into their operational models to assess the value of deploying similar instruments in future storms to improve intensity predictions. Similarly, efforts to integrate CBLAST results into the navy NOGAPS model effort and the Navy version of WRF. Special efforts will begin to asses the impact of the new air-sea parameterization schemes on hurricane intensity.

Acknowledgements. The authors and team of CBLAST investigators wish to thank the Office of Naval Research for supporting this work as a Departmental Research Initiative, award numbers N00014-01-F-009 (Black, Drennan, French), N0001401-1-0162 (Emanuel, Black), N00014-00-1-0894 (Terrill, Mellville), N00014-00-1-0893 (D'Asaro), N00014-02-1-0401 (Niiler) and N00014-01-F-0052 (Walsh), and to USWRP (NA17RJ1226, Drennan). EM-APEX floats were developed with an ONR-SBIR grant to Webb Research, Inc. We would like to thank NOAA Office of Atmospheric and Oceanic Research for P3 flight hour and expendable dropsonde support for two years and to the USWRP for CBLAST analysis support from 2005 to the present. We would especially like to thank the NESDIS Ocean Winds project and lead PI Paul Chang (also a CBLAST PI) for their sharing of flight hour and dropsonde resources, without which the extensive effort over three years would have been impossible. We would like to thank Frank Marks and the Hurricane Research Division staff for their infrastructure support for the NOAA aircraft field program effort, especially to Michael Black, Robert Rogers and Chris Landsea who served as Lead Project Scientist on many of the WP-3D flights. Special thanks is also due to James McFadden and the Aircraft Operations Center for their dedicated effort over four years to work with CBLAST PI's to test and install their instruments and in many cases to redesign their instruments for hurricane flight conditions. We especially thank Terry Lynch and Sean McMillan and the electrical engineering staff for their constant efforts to keep the computer and experimental hardware operating in hostile conditions and to Greg Bast and the aircraft flight engineer staff for their hard work to keep the aircraft in flight-ready status throughout the 3 years of active flights. Special thanks are due to Phil Hall, NOAA Corps, AOC and ARL, for his extensive efforts to certify airworthiness for the BAT probe. We would also like to thank Phil Kennedy and the flight crews for the expert piloting and navigation of the aircraft. Thanks are

especially due to Barry Damiano and Tom Shephard and the several flight directors who directed each CBLAST flight. Not one flight was cancelled and only one flight aborted due to mechanical problems. Special thanks is due to the 53rd Weather Reconnaissance Squadron of the Air Force Reserve Command for their extensive support of the buoy and float deployment effort, especially to Gen. Etheridge and Gen. Richard Moss who served as outgoing and incoming AFRC 403rd Wing Commanders during 2003-2004. We would especially like to thank Chief Robert E. Lee for supervising the air-drop training and bathroom renovations. Thanks to the many Air Force commands that participated in certifying the WC-130J, and individual platforms, to be deployed for airdrop capability. Finally special thanks are due to ONR CBLAST Program managers Simon Chang and Carl Friehe for actively helping to guide the program. Thanks is also due NOAA Deputy Assistant Administrator David Rogers for actively assisting in operational success of this experiment. Thanks is also due to Scott Sandgathe, Steve Tracton, Linwood Vincent, Theresa Paluszkiewicz and Ron Ferek for ONR management support.

References

Black, P. G., R. L. Elsberry and L. K. Shay, 1988: Airborne surveys of Ocean Current and temperature perturbations induced by hurricanes. *Adv. Underwater Technol., Ocean Sci. Engineer.*, **16**, 51-58.

Chen, S. S., W. Zhao, M. A. Donelan, J. F. Prices, E. J. Walsh, T. B. Sanford and H. L. Tolman, 2006: Fully Coupled Atmosphere-Wave-Ocean Modeling for Hurricane Research and Prediction: Results from CBLAST-Hurricane. Submitted to *BAMS*.

D'Asaro, E.A., 2003: Performance of autonomous Lagrangian floats. *J. Atmos. Oceanic Technol.*, 20, 896-911.

DeCosmo, J., K. B. Katsaros, S. D. Smith, R. J. Anderson, W. A. Oost, K. Bumke, and H. Chadwick, 1996: Air-sea exchange of water vapor and sensible heat: The humidity exchange over the sea (HEXOS) results. *J. Geophys. Res.,* **101** (C5), 12001-12016.

DeMaria, M., M. Mainelli, L.K. Shay, J.A. Knaff, and J. Kaplan, 2005: Further Improvements to the Statistical Hurricane Intensity Prediction Scheme (SHIPS), Wea. Forecasting, 20, 531-543.

Donelan, M. A., B. K. Haus, N. Reul, W. J. Plant, M. Stianssnie, H. C. Graber, O. B. Brown, E. S. Saltzman, 2004: On the limiting aerodynamic roughness of the ocean in very strong winds. *Geophys. Res. Lett.,* **31,** L18306.

Drennan, W. M., J. Zhang, J. R. French, C. McCormick and P. G. Black, 2006: Turbulent fluxes in the hurricane boundary layer, II. Latent heat flux, *J. Atmos. Sci.,* submitted.

Edson, J., T. Crawford, J. Crescenti, T. Farrar, J. French, N. Frew, G. Gerbi, C. Helmis, T. Hristov, D. Khelif, A. Jessup, H. Jonsson, M. Li, L. Mahrt, W. McGillis, A. Plueddemann, L. Shen, E. Skyllingstad, T. Stanton, P. Sullivan, J. Sun, J. Trowbridge, D.

Vickers, S. Wang, Q. Wang, R. Weller, J. Wilkin, D. Yu, and C. Zappa, 2006: The Coupled Boundary Layers and Air-Sea Transfer Experiment in Low Winds (CBLAST-LOW). Submitted to *BAMS*.

Emanuel, K. A., 1995: Sensitivity of tropical cyclones to surface exchange coefficients and a revised steady-state model incorporating eye dynamics. *J. Atmos. Sci.,* **52,** 3969-3976.

Emanuel, K. A., 2005: Increasing destructiveness of tropical cyclones over the past 30 years. Nature, 436, 686-688.

Esteban-Fernandez, D., S. Frazier, J. Carswell, P. Chang, P. Black and F. Marks, 2004: 3-D atmospheric boundary layer wind fields from Hurricanes Fabian and Isabel. *26th Conf. on Hurr. and Tropical Meteorol.*, AMS, Miami Beach, FL.

Fairall, C. W., E. F. Bradley, J. E. Hare, A. A. Grachev and J. B. Edson, 2003: Bulk parameterization of air-sea fluxes: updates and verification for the COARE algorithm. *J. Climate*, **16**, 571-591.

Foster, R. C., 2005: Why rolls are prevalent in the hurricane boundary layer. *J. Atmos. Sci.,* **62**, 2647-2661.

Franklin, J.L., C. J. McAdie, and M. B. Lawrence. 2003: Trends in Track Forecasting for Tropical Cyclones Threatening the United States, 1970–2001. Bull. Amer. Meteor. Soc., 84, 1197–1203.

French, J.R., W.M. Drennan, J. Zhang, and P.G. Black, 2006: Turbulent Fluxes in the Hurricane Boundary Layer, I. Momentum Flux. Submitted to *Journal of Atmospheric Science*.

Goldenberg, S.B., C.W. Landsea, A. M. Mestas-NuÑez, W. M. Gray, 2001: The Recent Increase in Atlantic Hurricane Activity: Causes and Implications. *Science* 293, 474-478.

Katsaros, K. B., P. W. Vachon, W. T. Liu, and P. G. Black, 2002: Microwave remote sensing of tropical cyclones from space. *J. Oceanogr.,* **58,** 137-151.

Kleiss, J. M., W. K. Melville, J. R. Lasswell, P. Matusov and E. Terrill, 2004: Breaking waves in hurricanes Isabel and Fabian. *26th Conf. on Hurr. and Tropical Meteorol.*, AMS, Miami Beach, FL.

Large, W. G., and S. Pond, 1981: Open ocean momentum flux measurements in moderate to strong winds. *J. Phys. Oceanogr.,* **11,** 324-336.

Lorsolo, S. and J. R. Schroeder, 2006: Small scale features observed in the boundary layer of Hurricanes Isabel (2003) and Frances (2004). *14th Conf. Interactions of the Sea and Atmosphere*, AMS, Atlanta.

Montgomery, M. T., M. Bell, S.D. Aberson, and M. Black, 2006: Superintense winds in Hurricane Isabel (2003). Part I: Mean vortex structure and maximum intensity estimates. Submitted to *Journal of the Atmospheric Sciences*

Morrison, I., S. Businger, F. Marks, P. Dodge and J. Businger, 2005: An observational case for the prevalence of roll vortices in the hurricane boundary layer, *J. Atmos. Sci.* **62**, 2662-2673.

Nystuen, J. A. and H. D. Selsor, 1997: Weather classification using passive acoustic drifters. *J. Atmos. and Oceanic Tech.*, **14**, 656-666.

Powell, M. D., P. J. Vickery, and T. A. Reinhold, 2003: Reduced drag coefficient for high wind speeds in tropical cyclones. *Nature*, **422**, 279-283.

Sanford, T. B., J. H. Dunlap, J. A. Carlson, D. C. Webb and J. B. Griton, 2005: Autonomous Velocity and Density Profiler: EM-APEX. Proceedings of the IEEE/OES Eighth

Working Conference on Current Measurement Technology, IEEE Cat No. 05CH37650, ISBN: 0-7803-8989-1, pp. 152-156

Smith, S. D., 1980: Wind stress and heat flux over the ocean in gale force winds. *J. Phys. Oceanogr.,* **10,** 709-726.

Smith, S.D., R.J. Anderson, W.A. Oost, C. Kraan, N. Maat, J. DeCosmo, K.B. Katsaros, K.L. Davidson, K. Bumke, L. Hasse and H.M. Chadwick, 1992: Sea surface wind stress and drag coefficients: the HEXOS results. *Bound. Layer Meteorol*. **60**, 109-142.

Uhlhorn, E. W., and P. G. Black, 2003: Verification of remotely sensed sea surface winds in hurricanes. *J. Atmos. Ocean. Technol.,* **20,** 99-116.

Wurman, J., and J. Winslow, 1998: Intense sub-kilometer-scale boundary layer rolls observed in Hurricane Fran. *Science*, **280,** 555-557.

Wright, C. W., E. J. Walsh, D. Vandemark, W. B. Krabill, S. H. Houston, M. D. Powell, P. G. Black, and F. D. Marks, 2001: Hurricane directional wave spectrum spatial variation in the open ocean. *J. Phys. Oceanogr.,* **31,** 2472-2488.

Table 1a. CBLAST Hurricane PI Team: functions and observable quantities, instrumentation and principal investigators (PIs)- **Aircraft Component**

No	Function	Instrument	PI	Affiliation
1	Chief Scientist, Flight Planning, Program Coordination	All	Peter Black	NOAA/AOML/HRD
2	Ocean Winds Lead Scientist, Sfc Wind Vector, SATCOM, Satellite Applications	IWRAP	Paul Chang	NOAA/NESDIS/ORA
3	Dropsondes, SST, Sfc Wind Speed	GPS sonde, AXBT, SFMR	Peter Black, Eric Uhlhorn	NOAA/AOML/HRD
4	Sea spray, particle spectrometer	CIP	Chris Fairall	NOAA/ESRL/ETL
5	Sea spray, particle velocimeter	PDA	William Asher	U. Washington/APL
6	Extreme wind sfc flux, theory	Dropsonde	Kerry Emanuel	MIT
7	Surface waves	SRA	Ed Walsh	NASA/Goddard
8	Momentum, sensible heat flux	BAT	Jeff French	NOAA/ARL; U. Wyoming
9.	Moisture flux	LICOR	William Drennan	U. Miami/RSMAS
10.	Surface wind vector, continuous PBL wind profiles	IWRAP, USFMR	Stephen Frasier, James Carswell, Daniel Esteban, Rob Contreras	UMASS/ MIRSL
11.	Surface wave breaking, foam coverage	MASS VIS camera, IR camera	Ken Melville, Eric Terrill	UCSD/SCRIPPS

Table 1b. CBLAST Hurricane PI Team: functions and observable quantities, instrumentation and principal investigators (PIs)- **Drifter/ Float Component**

No	Function	Instrument	PI	Affiliation
1	Ocean mixing, gas exchange	Lagrangian floats	Eric D'Asaro	U. Washington/APL
2	Ocean current, temperature and salinity profiling	EM-APEX floats	Tom Sanford	U. Washington/APL
3	Ocean acoustics, surface waves, ocean temperature profiles	ARGO/SOLO floats	Eric Terrill	UCSD/SCRIPPS
4	SST, Sfc wind vector, ocean acoustics, surface air pressure	SVP/ADOS drifters	Peter Niiler, William Scuba Jan Morzel	UCSD/SCRIPPS
5	Satellite ocean heat content, buoy archive	Satellite altimeters	Gustavo Goni	NOAA/AOML/PHOD

Table 2: List of acronyms

ADOS	Autonomous Drifting Ocean Stations
AFRC	Air Force Reserve Command
AOC	Aircraft Operations Center
AOML	Atlantic Oceanographic and Meteorological Laboratory
APL	Applied Physics Laboratory
AXBT	Airborne Expendable Bathythermograph
BAT	Best Aircraft Turbulence
CAMEX	Convection And Moisture Experiment
CBLAST	Coupled Boundary Layer Air-Sea Transfer
CIP	Cloud Imaging Probe
COAMPS	Coupled Ocean Atmosphere Mesoscale Prediction System
COARE	Coupled Ocean-Atmosphere Response Experiment
DSD	Drop size distribution
EM-APEX	Electro-Magnetic Autonomous Profiling Explorer
EMC	Environmental Modeling Center
ETL	Environmental Technology Laboratory
FRD	Field Research Division
FSSP	Forward Scattering Spectrometer Probe
HEXOS	Humidity Exchange Over the Sea
HFPP	Hurricane Field Program Plan
HRD	Hurricane Research Division
HWIND	HRD Hurricane wind analysis
HWRF	Hurricane Weather Research and Forecasting
IWRAP	Integrated Wind and Rain Atmospheric Profiler
MASS	Mass spectrometer
NESDIS	National Environmental Satellite Data Information Service
NOGAPS	Navy Operational Global Atmospheric Prediction System
NRL	Naval Research Laboratory
OAR	Office of Oceanic and Atmospheric Research
ONR	Office of Naval Research
PDA	Precipitation Detection Algorithm
PHOD	Physical Oceanography Division
SATCOM	Satellite Communications System
SBIR	Small Business Innovative Research
SFMR	Stepped Frequency Microwave Radiometer
SOLO	Sounding Oceanographic Lagrangian Observer
SRA	Scanning Radar Altimeter
TA	Tail Doppler radar
TOGA	Tropical Ocean Global Atmosphere
UM	University of Miami
UMASS	University of Massachusetts
USWRP	United States Weather Research Program
UW	University of Washington
WRS	Weather Reconnaissance Squadron

Table 3 –Oceanographic Platforms Deployed in CBLAST Hurricane

	MiniMet	**ADOS**	**EM-APEX**	**Lagrangian**	**SOLO**
Type	Drifter	Drifter	Float	Float	Float
Measurements	SST Air Pressure Wind Speed Wind direction Position	SST Air Pressure Wind Speed Wind Direction Temperature 0-120m Position	Temperature Salinity Pressure Velocity Position	Temperature Salinity Pressure Gas Tension Oxygen Position	Temperature Salinity Pressure Oxygen Sound 0-50kHz Wave height Position
Satellite	Argos – 1 way	Argos – 1 way	Iridium-2 way	Iridium – 2 way	Orbcomm-2 way
2004 Deployed	8			4	2
2005 Deployed	30	16	3	2	9

Figure Captions

Figure 1. CBLAST survey pattern showing planned expendable probe deployments along a 'figure 4' pattern relative to the storm's eyewall and rainband features. Location of planned stepped-descent patterns to measure boundary layer fluxes is shown schematically.

Figure 2. Vertical alignment of stepped descent flight legs along with expendable probe location along the 25 nmi (40km) leg length.

Figure 3. Deployment of a drifting buoy package from an AFRC WC-130J aircraft.

Figure 4. CBLAST aircraft fleet in St. Croix consisting of two NOAA WP-3D aircraft and the AFRC WC-130J aircraft. The latter was used to air-deploy the drifters and floats ahead of Hurricanes Fabian (2003) and Frances (2004).

Figure 5. NOAA WP-3D crew and scientists in front of one of the WP-3D aircraft.

Figure 6. Location of the BAT turbulence probe and LICOR fast response humidity probe on the WP-3D aircraft.

Figure 7. CBLAST stepped descent flight patterns flown in Hurricanes Fabian and Isabel in 2003, plotted in storm-relative coordinates, with the storm motion indicated by the arrow (up). Circles are shown at 100 km intervals.

Figure 8. Drag coefficient estimates derived from CBLAST stepped-descent flight legs in Hurricanes Fabian and Isabel (2003). The asterisks represent average values in 2.5 m/s bins. The red squares are from flight legs in the right-front quadrant of the storms, green plus signs from the right-rear quadrant and the blue diamonds from the left-front quadrant. The dotted line represents Large and Pond 1981 (LP) extrapolated to 35 m/s winds. Peak winds for LP were 22 m/s.

Figure 9. Humidity exchange coefficient (Dalton Number) estimates derived from CBLAST stepped-descent flight legs in Hurricanes Fabian and Isabel (2003). The asterisks represent average values in 2.5 m/s bins. The red squares are from flight legs in the right-front quadrant of the storms, green plus signs from the right-rear quadrant and the blue diamonds from the left-front quadrant. The dotted line represents a mean for the range of wind speeds from 15 to 32 m/s.

Figure 10. Drag coefficient C_D (left axis) and Dalton number C_E (right axis) as a function of wind speed. Plotted are CBLAST values of C_D (red diamonds) and C_E (blue inverted triangles) compared with recent C_D estimates from Powell et al, 2003 (black line, open triangles), Donelan et al., 2004 (blue line, open triangles), an average of Large and Pond, 1981 and Smith, 1980 (heavy black line) and HEXOS for ocean depths of 18 (dotted line) and 30 m (dashed line) and C_E values for HEXOS (Decosmo et al., 1996- black crosses) and TOGA/COARE (Fairall, et al., 2003- black solid triangles). Also shown are very preliminary C_D and C_E budget

estimates (dotted pink and dash-dotted light blue, respectively) from Emanuel and Fairall ongoing studies.

Figure 11. Ratio of Dalton number to drag coefficient derived from CBLAST measurements (circles with vertical lines indicating standard error) as well as an average of prior values below 20 m/s from HEXOS (DeCosmo et al., 1996; Smith et al., 1992, dashed line) and TOGA-COARE-3.0 (Fairall et al, 2003, solid line). Estimated value based on budget estimate (Emanuel, 2004) at winds near 70 m/s is shown with a square. Interpolated estimates from Fairall estimate of spray effects shown with asterisks. The thin horizontal line is the 0.75 threshold for TC development proposed by Emanuel, 1996.

Figure 12. Swath of wave elevations from SRA during Fabian from 200 m flight altitude during Fabian, 2003. Scale of aircraft is shown at 1 km along track, 0.2 km cross track position.

Figure 13. Analysis of SRA swell direction of propagation, wave height (dashed black contours) and wave steepness (solid blue contours) for Hurricane Bonnie.

Figure 14. The center of the figure shows wind speed contours (m/s) from the HRD HWIND surface wind analysis- based mainly on SFMR surface wind speed measurements in Hurricane Ivan at 2230 UTC on 14 September 2004 for a 2° box in latitude and longitude centered on the eye. Arrow at the center indicates Ivan's direction of

motion (330º). The storm-relative locations of twelve 2D surface wave spectra measured by the SRA are indicated by the black dots. The spectra have nine solid contours linearly spaced between the 10% and 90% levels relative to the peak spectral density. The dashed contour is at the 5% level. The outer solid circle indicates a 200 m wavelength and the inner circle indicates a 300 m wavelength. The dashed circles indicate wavelengths of 150, 250, and 350 m (outer to inner). The thick line at the center of each spectrum points in the downwind direction, with its length proportional to the surface speed. The upper number at the center of each spectrum is the significant wave height and the lower number is the distance from the center of the eye. The average radial distance for the twelve spectral locations is 80 km. The SRA data which produced the spectra were collected between 2030 UTC on 14 September and 0330 UTC on 15 September.

Figure 15. ENVISAT SAR image (top) from right-front quadrant of Hurricane Fran, similar to that obtained for Hurricane Isidore, 2002. Spectrum of wavelengths from RADARSAT image of Hurricane Isidore, 2002. Arrow indicates peak in aircraft-derived spectrum in Fig. 16.

Figure 16. Spectrum of vertical momentum flux along a 300 m altitude radial flight leg into Hurricane Isidore, 2002.

Figure 17. Drawings of the three varieties of floats and a surface drifter as deployed into Hurricane Frances. Schematic depicts operations in Hurricane Frances (2004).

Figure 18. Hurricane Frances float and drifter array. Heavy line shows storm track, labeled by day (245.00 = Aug. 31, 2004 00Z). Colors indicate type of instrument. Instrument tracks are plotted from deployment to day 246.5. Deployment position is indicated by black symbol.

Figure 19. Significant surface wave height and bubble cloud depth measured by the 9 SOLO floats and wind speed at the float location from HWINDS analysis. Time axis is hours from time of maximum wind at each float.

Figure 20. Evolution of the temperature structure of the upper ocean near the radius of maximum winds of Hurricane Frances. a) Wind speed and atmospheric pressure from HRD HWIND analysis at the two Lagrangian floats. b) Temperature contours (black and gray), trajectories of Lagrangian floats (red and blue) and depth of the mixed layer measured (magenta) and from a vertical heat budget (yellow dashed).

Figure 21. U and V components of the currents superimposed upon the ocean vertical temperature structure together with Ocean Heat Content (OHC). Center of the storm passed at approximately 1700 UTC on Sept 1.

Figure 22. Cooling of SST beneath hurricane Frances in storm-centered coordinate system. White dots show storm-relative locations of float and drifter data. Storm motion is to left. Colors show mapped SST change from pre-storm value. Contours show wind speed.

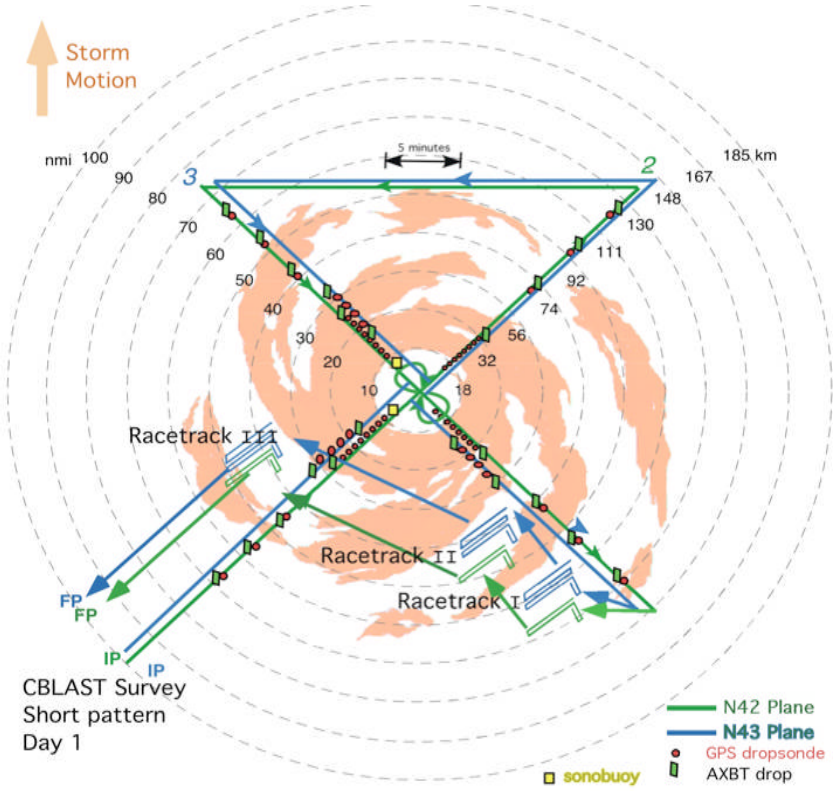

Figure 1. CBLAST survey pattern showing planned expendable probe deployments along a ‘figure 4’ pattern relative to the storm’s eyewall and rainband features. Location of planned stepped-descent patterns to measure boundary layer fluxes is shown schematically.

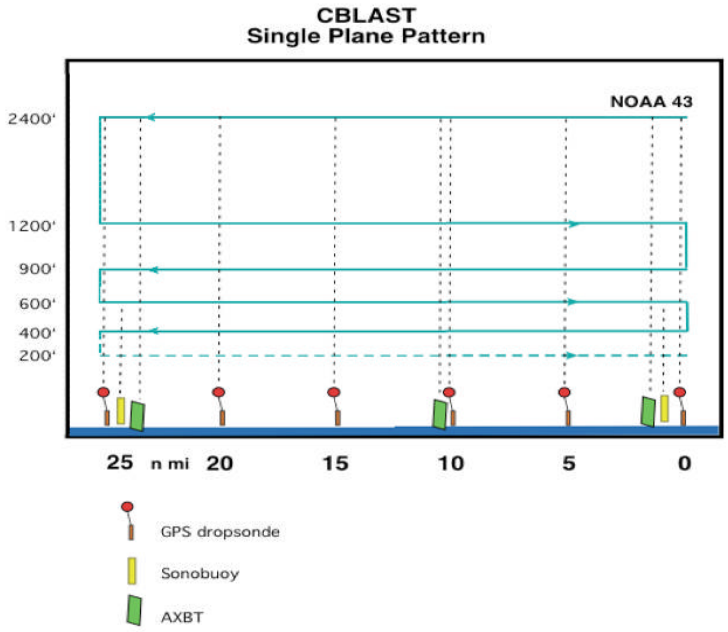

Figure 2. Vertical alignment of stepped descent flight legs along with expendable probe location along the 25 nmi (40km) leg length.

Figure 3. Deployment of a drifting buoy package from an AFRC WC-130J aircraft.

Figure 4. CBLAST aircraft fleet in St. Croix consisting of two NOAA WP-3D aircraft and the AFRC WC-130J aircraft. The latter was used to air-deploy the drifters and floats ahead of Hurricanes Fabian (2003) and Frances (2004).

Figure 5. NOAA WP-3D crew and scientists in front of one of the WP-3D aircraft.

Figure 6. Location of the BAT turbulence probe and LICOR fast response humidity probe on the WP-3D aircraft.

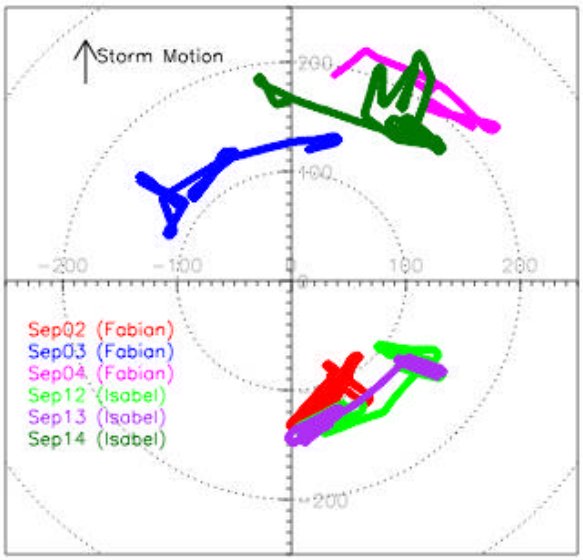

Figure 7. CBLAST stepped descent flight patterns flown in Hurricanes Fabian and Isabel in 2003, plotted in storm-relative coordinates, with the storm motion indicated by the arrow (up). Circles are shown at 100 km intervals.

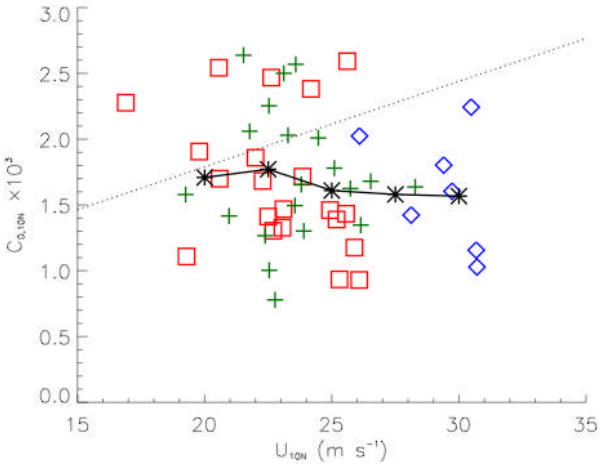

Figure 8. Drag coefficient estimates derived from CBLAST stepped-descent flight legs in Hurricanes Fabian and Isabel (2003). The asterisks represent average values in 2.5 m/s bins. The red squares are from flight legs in the right-front quadrant of the storms, green plus signs from the right-rear quadrant and the blue diamonds from the left-front quadrant. The dotted line represents Large and Pond, 1981 (LP) extrapolated to 35 m/s winds. Peak winds for LP were 22 m/s.

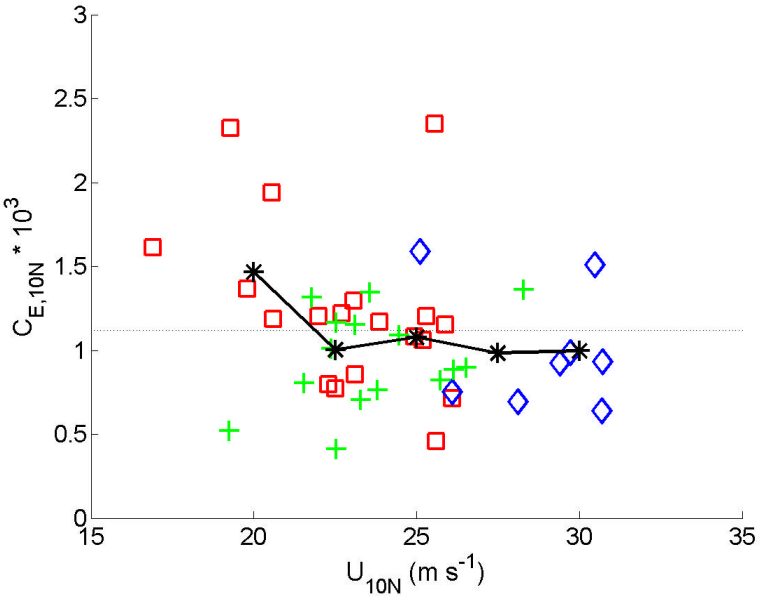

Figure 9. Humidity exchange coefficient (Dalton Number) estimates derived from CBLAST stepped-descent flight legs in Hurricanes Fabian and Isabel (2003). The asterisks represent average values in 2.5 m/s bins. The red squares are from flight legs in the right-front quadrant of the storms, green plus signs from the right-rear quadrant and the blue diamonds from the left-front quadrant. The dotted line represents a mean for the range of wind speeds from 15 to 32 m/s.

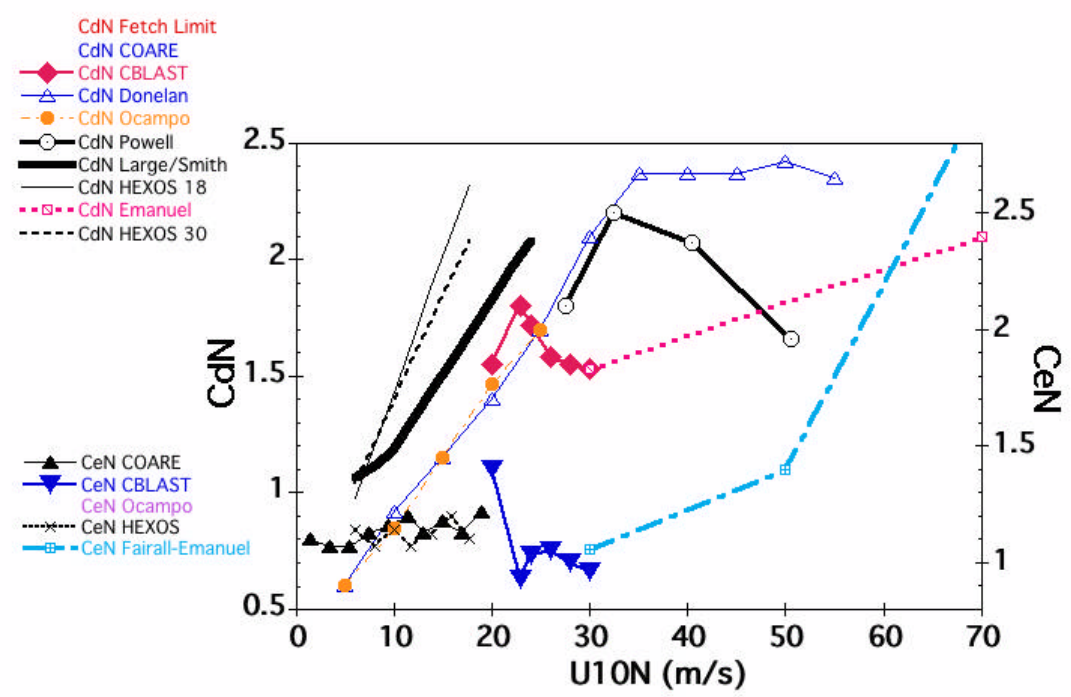

Figure 10. Drag coefficient C_D (left axis) and Dalton number C_E (right axis) as a function of wind speed. Plotted are CBLAST values of C_D (red diamonds) and C_E (blue inverted triangles) compared with recent C_D estimates from Powell et al, 2003 (black line, open triangles), Donelan et al., 2004 (blue line, open triangles), an average of Large and Pond, 1981 and Smith, 1980 (heavy black line) and HEXOS for ocean depths of 18 (dotted line) and 30 m (dashed line) and C_E values for HEXOS (Decosmo et al., 1996- black crosses) and TOGA/COARE (Fairall, et al., 2003- black solid triangles). Also shown are very preliminary C_D and C_E budget estimates (dotted pink and dash-dotted light blue, respectively) from Emanuel and Fairall ongoing studies.

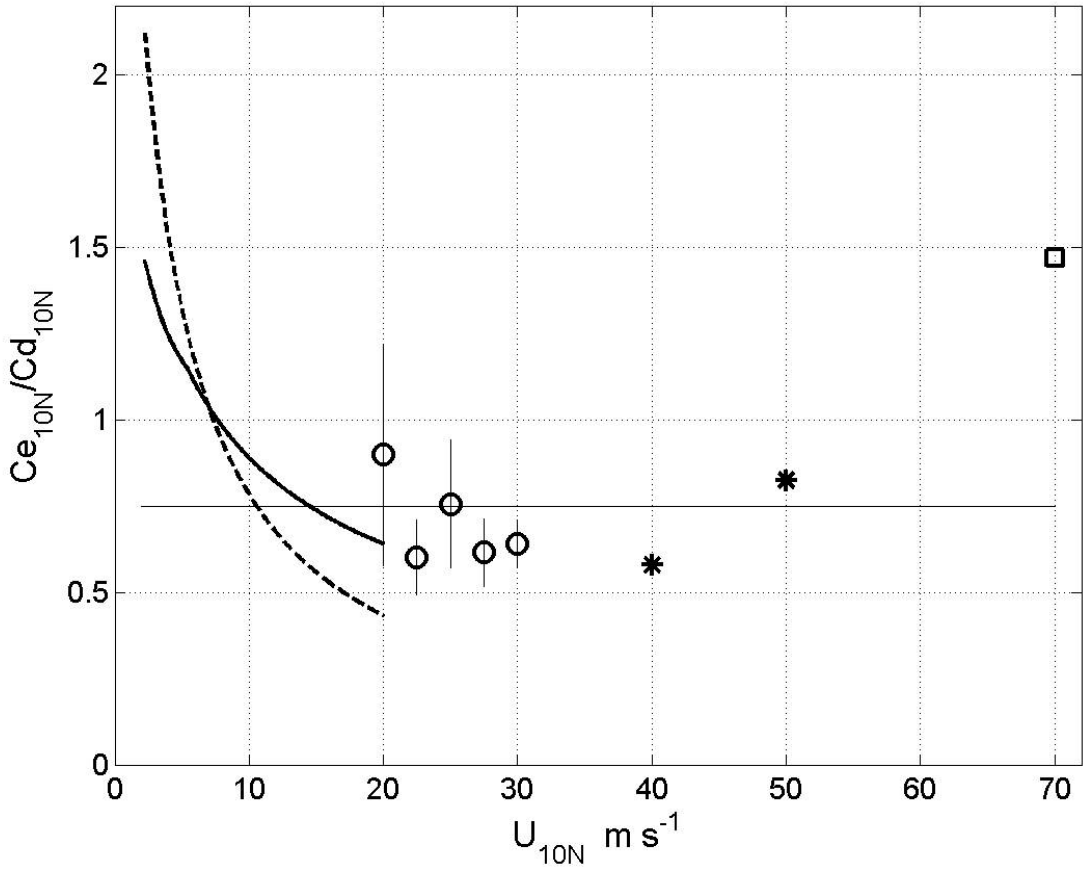

Figure 11. Ratio of Dalton number to drag coefficient derived from CBLAST measurements (circles with vertical lines indicating standard error) as well as an average of prior values below 20 m/s from HEXOS (DeCosmo et al., 1996; Smith et al, 1992, dashed line) and TOGA-COARE 3.0 (Fairall et al 2003, solid line). Estimated value based on budget estimate (Emanuel, 2004) at winds near 70 m/s is shown with a square. Interpolated estimates from Fairall estimate of spray effects shown with asterisks. The thin horizontal line is the 0.75 threshold for TC development proposed by Emanuel, 1996.

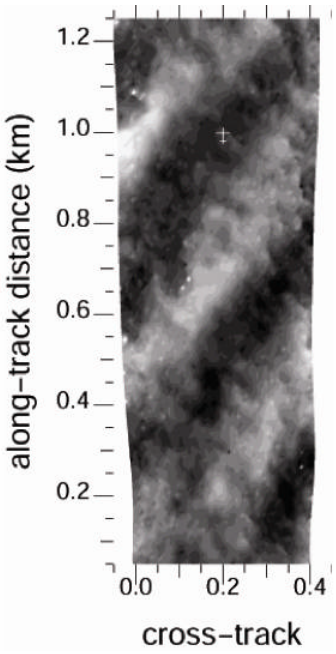

Figure 12. Swath of wave elevations from SRA during Fabian from 200 m flight altitude during Fabian, 2003. Scale of aircraft is shown at 1 km along track, 0.2 km cross track position.

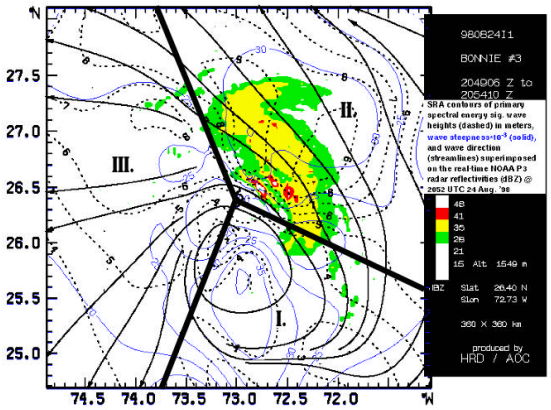

Figure 13. Analysis of SRA swell direction of propagation, wave height (dashed black contours) and wave steepness (solid blue contours) for Hurricane Bonnie.

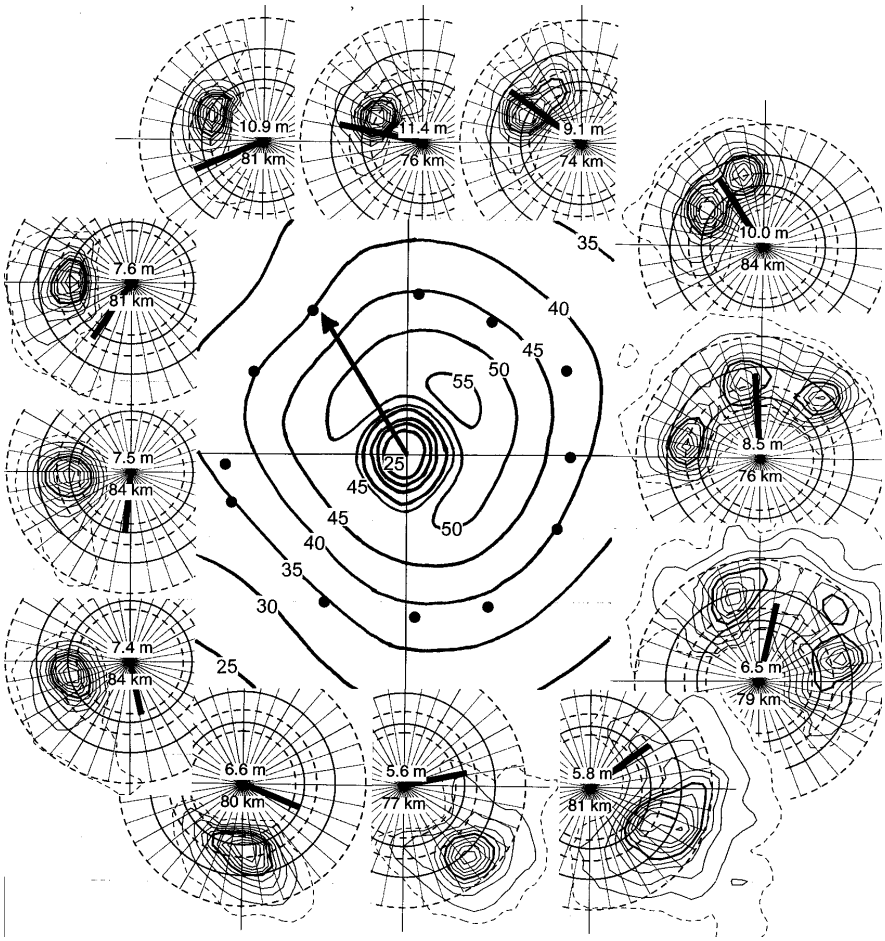

Figure 14. The center of the figure shows wind speed contours (m/s) from the HRD HWIND surface wind analysis- based mainly on SFMR surface wind speed measurements in Hurricane Ivan at 2230 UTC on 14 September 2004 for a 2° box in latitude and longitude centered on the eye. Arrow at the center indicates Ivan's direction of motion (330º). The storm-relative locations of twelve 2D surface wave spectra measured by the SRA are indicated by the black dots. The spectra have nine solid contours linearly spaced between the 10% and 90% levels relative to the peak spectral density. The dashed contour is at the 5% level. The outer solid circle indicates a 200 m wavelength and the inner circle indicates a 300 m wavelength. The dashed circles indicate wavelengths of 150, 250, and 350 m (outer to inner). The thick line at the center of each spectrum points in the downwind direction, with its length proportional to the surface speed. The upper number at the center of each spectrum is the significant wave height and the lower number is the distance from the center of the eye. The average radial distance for the twelve spectral locations is 80 km. The SRA data which produced the spectra were collected between 2030 UTC on 14 September and 0330 UTC on 15 September.

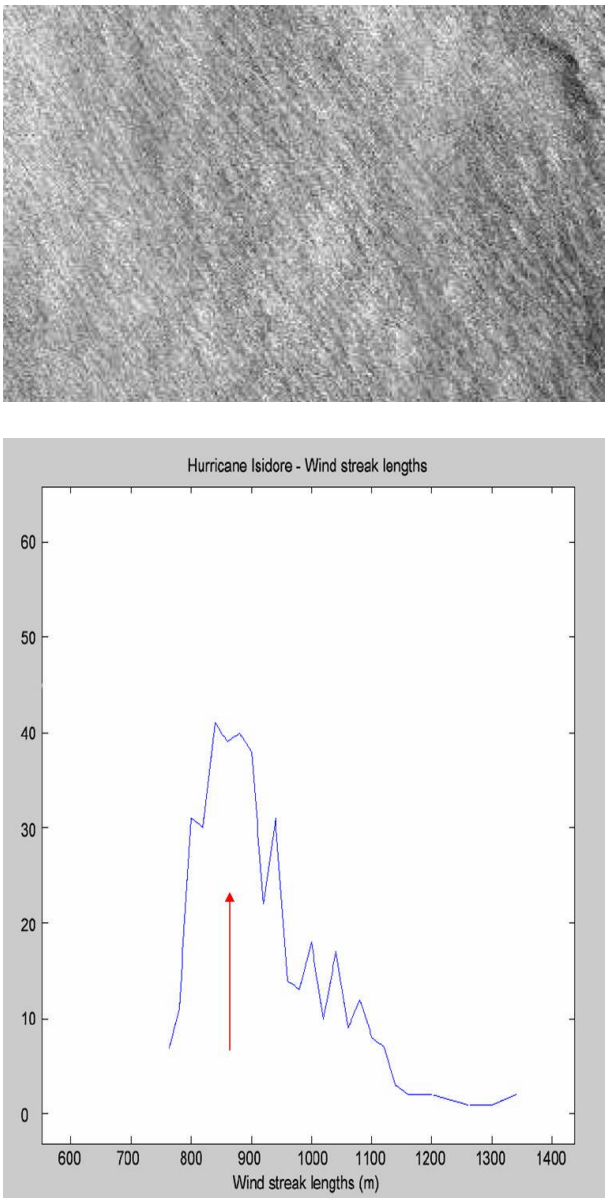

Figure 15. ENVISAT SAR image (top) from right-front quadrant of Hurricane Fran, similar to that obtained for Hurricane Isidore, 2002. Spectrum of wavelengths from RADARSAT image of Hurricane Isidore, 2002. Arrow indicates peak in aircraft-derived spectrum in Fig. 16.

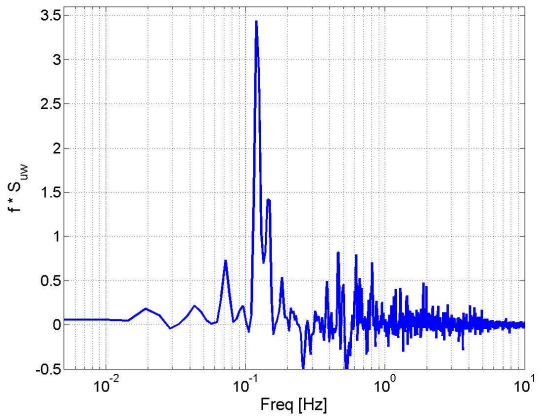

Figure 16. Spectrum of vertical momentum flux along a 300 m altitude radial flight leg into Hurricane Isidore, 2002.

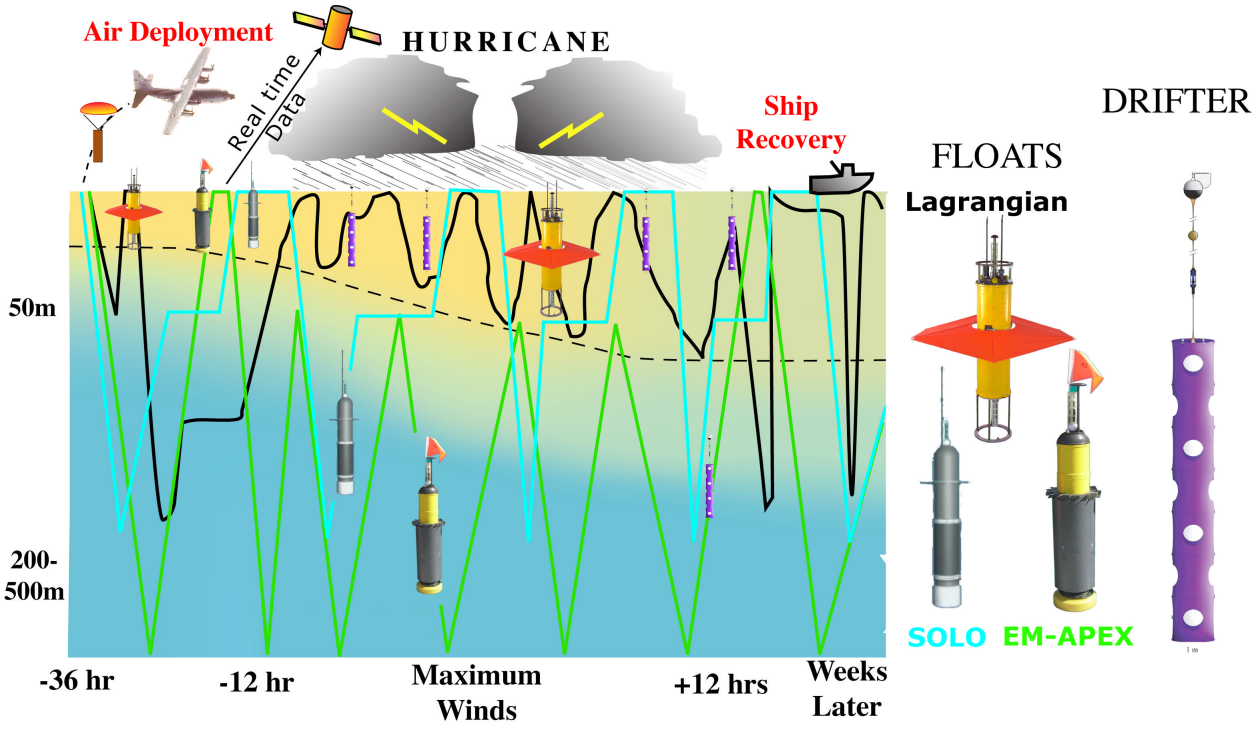

Figure 17. Drawings of the three varieties of floats and a surface drifter as deployed into Hurricane Frances. Schematic depicts operations in Hurricane Frances (2004).

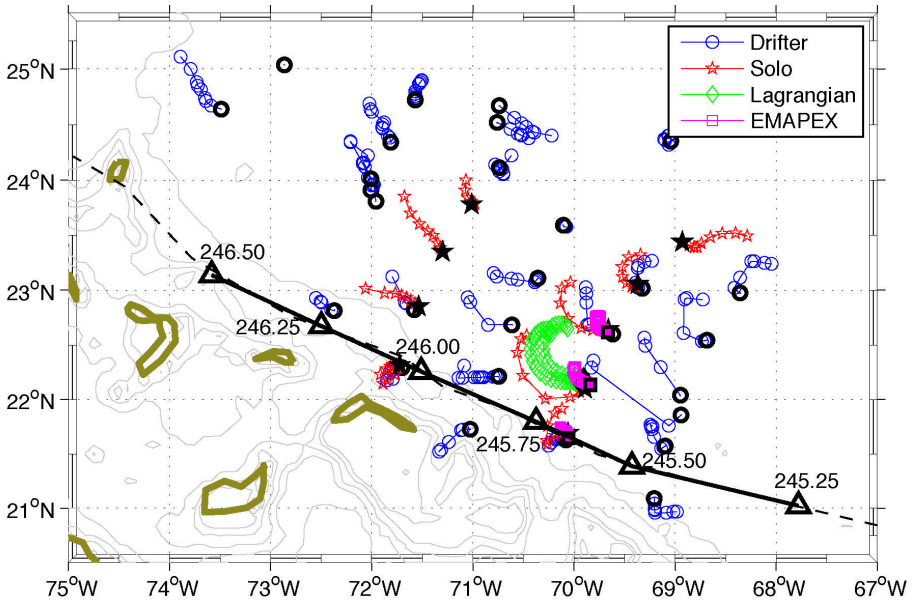

Figure 18. Hurricane Frances float and drifter array. Heavy line shows storm track, labeled by day (245.00 = Aug. 31, 2004 00Z). Colors indicate type of instrument. Instrument tracks are plotted from deployment to day 246.5. Deployment position is indicated by black symbol.

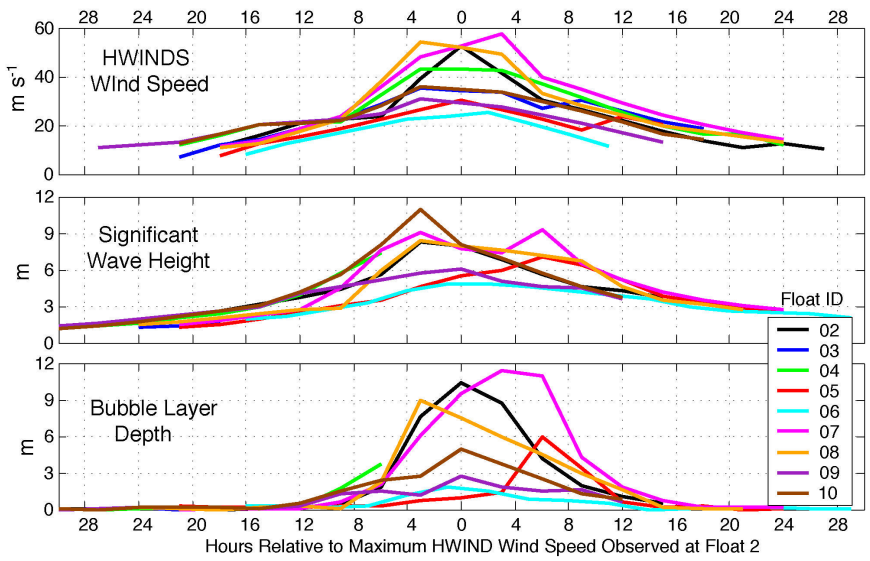

Figure 19. Significant surface wave height and bubble cloud depth measured by the 9 SOLO floats and wind speed at the float location from HWINDS analysis. Time axis is hours from time of maximum wind at each.

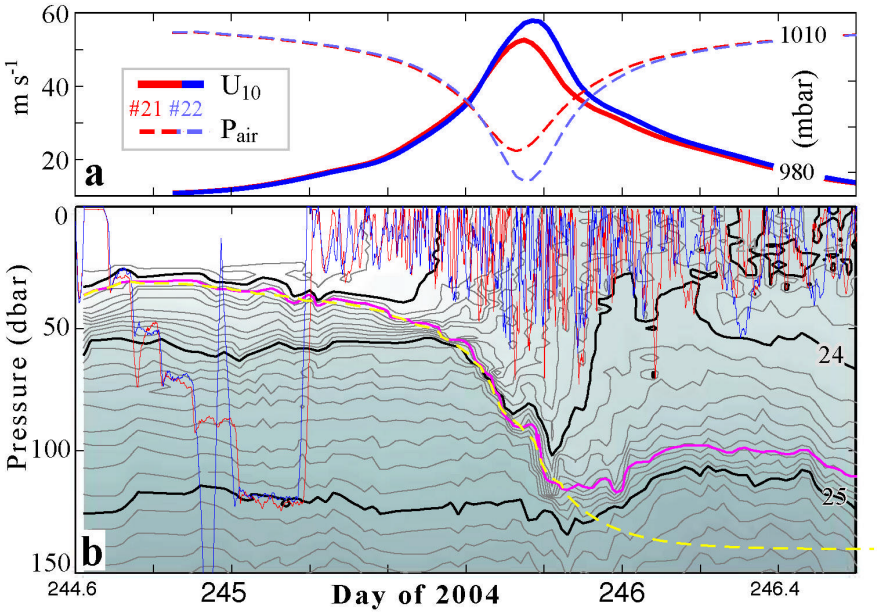

Figure 20. Evolution of the temperature structure of the upper ocean near the radius of maximum winds of Hurricane Frances. a) Wind speed and atmospheric pressure from HRD HWIND analysis at the two Lagrangian floats. b) Temperature contours (black and gray), trajectories of Lagrangian floats (red and blue) and depth of the mixed layer measured (magenta) and from a vertical heat budget (yellow dashed).

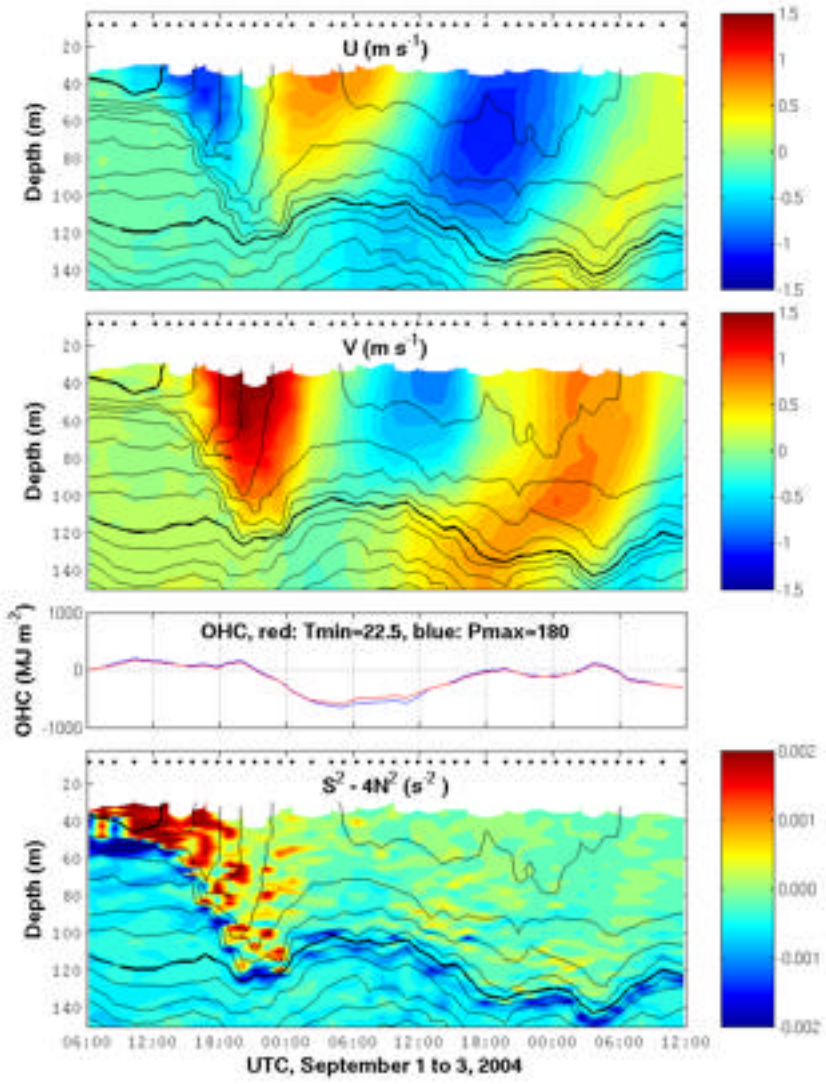

Figure 21. U and V components of the currents superimposed upon the ocean vertical temperature structure together with Ocean Heat Content (OHC). Center of the storm passed at approximately 1700 UTC on Sept 1.

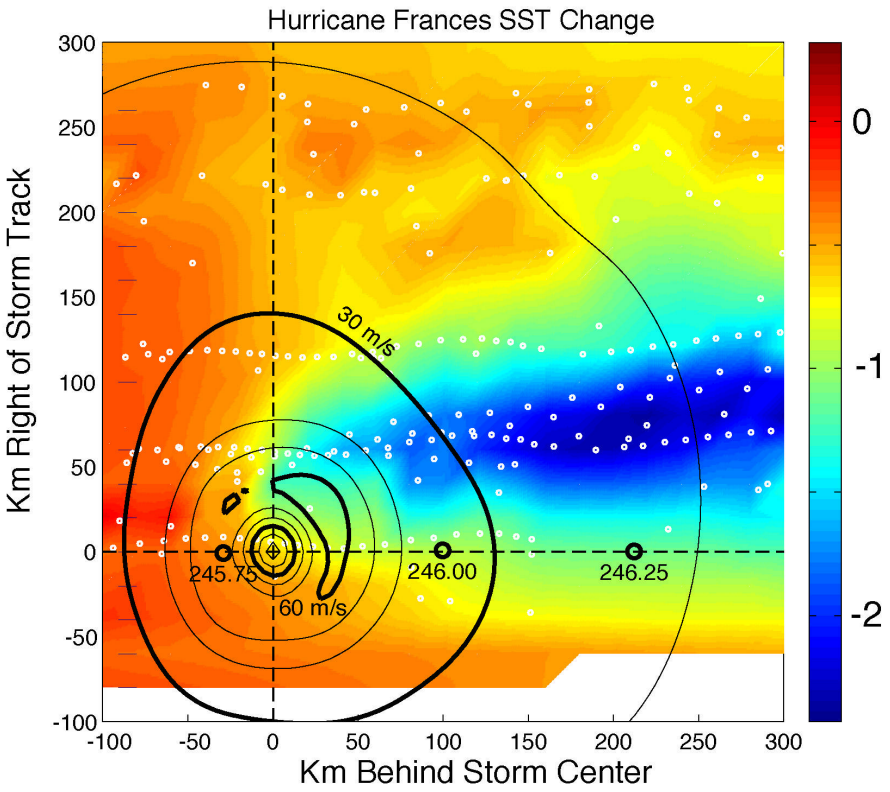

Figure 22. Cooling of SST beneath hurricane Frances in storm-centered coordinate system. White dots show storm-relative locations of float and drifter data. Storm motion is to left. Colors show mapped SST change from pre-storm value. Contours show wind speed.